Feasibility of H_2O_2 cleaning for forward osmosis membrane treating landfill leachate

Ibrar Ibrar[1], Sudesh Yadav[1], Namuun Ganbat[1], Akshaya K Samal[2], Ali Altaee[1]*, John L Zhou[1], Tien Vinh Nguyen[1],

1: Centre for Green Technology, School of Civil and Environmental Engineering, University of Technology Sydney, 15 Broadway, NSW, 2007, Australia

2: Centre for Nano and Material Science (CNMS), Jain University, India

*Corresponding author email address: ali.altaee@uts.edu.au

*Corresponding author phone number: +61 295149668

Abstract

This study reports landfill leachate treatment by the forward osmosis (FO) process using hydrogen peroxide (H_2O_2) for membrane cleaning. Although chemical cleaning is an effective method for fouling control, it could compromise membrane integrity. Thus, understanding the impact of chemical cleaning on the forward osmosis membrane is essential to improving the membrane performance and lifespan. Preliminary results revealed a flux recovery of 98% in the AL-FS mode (active layer facing feed solution) and 90% in the AL-DS (draw solution faces active layer) using 30% H_2O_2 solution diluted to 3% by pure water. The experimental work investigated the effects of chemical cleaning on the polyamide active and polysulfone support layers since the FO membrane could operate in both orientations. Results revealed that polysulfone support layer was more sensitive to H_2O_2 damage than the polyamide active at a neutral pH. The extended exposure of thin-film composite (TFC) FO membrane to H_2O_2 was investigated, and the active layer tolerated H_2O_2 for 72 hours, and the support layer for only 40 hours. Extended operation of the TFC FO membrane in the AL-FS based on a combination of physical (hydraulic flushing with DI water) and H_2O_2 was reported, and chemical cleaning with H_2O_2 could still recover 92% of the flux.

Keywords: hydrogen peroxide, landfill leachate treatment, membrane damage, fouling, membrane oxidation.

1. Introduction

Sanitary landfills are considered an effective way for disposal of solid waste (Atmaca, 2009; Renou et al., 2008a). Comparative studies revealed that the sanitary landfill method is the most economic method of eliminating solid urban waste (Renou et al., 2008b). Despite being

effective, these landfill sites generate undesirable and hazardous leachate wastewater when rainwater percolates through the dumping site. The landfill leachate wastewater is regarded as a serious environmental threat due to the existence of various hazardous organic and inorganic compounds (Danley-Thomson et al., 2020; Ghanbari et al., 2020; Reshadi et al., 2020). The disposal of landfill leachate wastewater is a challenging problem that has been encountered by the municipal waste management industry. The composition of landfill leachate varies from site to site (Abbas et al., 2009; Renou et al., 2008a), which makes the treatment process of landfill leachate a formidable challenge. If not appropriately treated, landfill leachate can contaminate both groundwater and surface water; therefore, it requires an efficient treatment process.

Currently, biological treatments (e.g. aerobic, anaerobic, physical/chemical) and membrane processes (nanofiltration and reverse osmosis), or a combination of different processes (Marttinen et al., 2002; Rautenbach and Mellis, 1994; Trebouet et al., 2001) are the dominant processes for landfill leachate treatment. Biological processes are usually used to treat leachate because they are simple and economical (Peng, 2017). However, authority's stricter environmental regulations make biological processes incompetent, as they cannot satisfy the specifications required for discharge. A significant increase in pressure-driven membrane technologies has been noticed compared to biological treatment methods in recent years (Bhol et al., 2021; Renou et al., 2008a). Among membrane processes, reverse osmosis (RO) (43 RO plants) and nanofiltration (NF) treatment of landfill leachate have been widely used worldwide (Trebouet et al., 2001). However, membrane fouling and large concentrate generation are critical issues in the RO process (Renou et al., 2008a), and the NF membrane exhibits low permeability. For instance, Li et al. (2009) studied the tertiary treatment of landfill wastewater using thin-film composite (TFC) RO membranes, achieving a water flux of 6.5 Lm^2h^{-1} with a 53.4% recovery rate; however, membrane fouling resulted in a complete loss of permeability after two weeks. The RO technology also demands intensive pre-treatment of the FS and membrane cleaning to overcome fouling, (Renou et al., 2008a) and is therefore not considered affordable. In another study, a composite graphene-oxide (GO) NF membrane was used for landfill leachate treatment. Although an 86.5% to 99.8% rejection rate was achieved, low membrane permeability (6.93 to 2.05 LMH) was a significant challenge (Yadav et al., 2020a).

Forward osmosis (FO) is an alternative membrane technology for reducing the volume of landfill leachate wastewater (Ibrar et al., 2020a; Ibrar et al., 2020b; Yadav et al., 2020b) and freshwater recovery (Iskander et al., 2019). In the FO, a concentrated DS will extract freshwater from landfill leachate for volume reduction. Then, the diluted DS will either be treated for freshwater water production or safe discharge. For a successful FO treatment, membrane fouling control and cleaning strategies will inevitably achieve a high recovery rate. Dong et al. (2014)) used a cellulose triacetate (CTA) membrane to treat MBR (membrane bioreactor) landfill wastewater; however, membrane chemical cleaning was unavoidable. Chemical cleaning was conducted using Alconox as a cleaning agent; however, Alconox is only feasible for CTA membrane and detrimental to TFC membranes (Wang et al., 2015). Aftab et al. (2019) used 0.1M NaOH to clean a CTA FO membrane treating landfill wastewater due to physical cleaning failure to restore water flux. Previous studies on the FO process for landfill leachate treatment demonstrated that H_2O_2 could be an alternative to acid and alkaline cleaning of the membrane, but CTA membrane damage was observed on the active and support layers after the H_2O_2 cleaning (Ibrar et al., 2020b).

Compared to CTA membranes, thin-film composite (TFC) FO membranes are broadly employed in desalination and wastewater treatment systems because of the high permeation water flux and rejection of ions. Also, CTA membranes are sensitive to oxidants and operate within a narrow pH range (Farooque et al., 1999). In contrast, TFC membranes are relatively tolerant of oxidant damage and tolerate a pH range from 2 to 12. H_2O_2 is environmentally safe, and it can efficiently remove foulants (almost 100%) from the membrane surface, compared to chemical cleanings such as citric acid, hydrochloric acid (HCl), sodium hydroxide (NaOH), sodium dodecyl sulphate (SDS), and disodium ethylenediaminetetraacetate (Ibrar et al., 2020b; Wang et al., 2017). Other oxidizing agents such as sodium hypochlorite (NaOCl) can react with organics, generating halogenated by-products that are potentially more toxic to the environment (Cai et al., 2016; Li et al., 2019).

In this study, the FO process was applied for landfill leachate treatment using an H_2O_2 cleaning agent. For the first time, the polyamide and polysulfone (PSf) support layer of TFC FO membrane tolerance to long-term exposure to H_2O_2 was experimentally investigated. There is no systematic study that has reported the tolerance of TFC FO membrane over an extended period to H_2O_2. Firstly, the TFC membrane performance was investigated for dewatering of

landfill leachate in the AL-FS (leachate feed against the active layer) and the AL-DS (DS against the active layer). Secondly, in separate experiments, the TFC membrane tolerance to H_2O_2 was investigated for the polyamide active layer and the PSf support layer in the long term. A 4-day continuous operation with H_2O_2 cleaning was performed to calculate the permeation flux and the membrane rejection rate at the end of the experiments.

2. Materials

2.1. Leachate sampling and chemicals

The landfill leachate samples were procured from the Hurstville Golf course located at Peakhurst, Sydney, Australia, and employed as a FS (FS). The DS (DS) was 0.6 M NaCl simulating the osmotic pressure of real seawater. In a long filtration test, the DS was 1M NaCl solution to avoid a significant dilution of the DS. Analytical grade H_2O_2 (30% w/w) was purchased from Merck Millipore, and was used as a cleaning agent in all the fouling experiments.

2.2. FO membrane

This study used a TFC (thin-film composite) membrane, Toray Chemical (South Korea), in the FO tests. This membrane consists of a polyamide active layer and a PSf porous support layer (Nguyen et al., 2019). Detailed intrinsic properties of this membrane were determined and are summarised in Table S.1 (Supplementary information). The virgin membranes were placed in DI water for at least 24 hours before using in the experiments, to ensure complete wetting.

2.3. FO laboratory setup and experimental methodology

A schematic diagram of the FO cell termed CF042D by the manufacturer (Sterlitech Corporation, USA) can be found in our previous study (Ibrar et al., 2020a). The cell features a membrane area of 42 cm^2. The feed and DS were pumped using two gear pumps at a rate of 2 Litres/minute. Two- flow meters (FF-550) were connected to the FO cell to monitor the feed and DS flow rate. The FS was placed on a balance (EK-15L) connected to a computer that recorded the weight change in the FS. The data obtained from the computer (grams) was converted to the volume (V), and the water flux was calculated using equation 1.

$$J_w = \frac{(\Delta V)}{A*t} \quad (1)$$

In equation 1 ΔV represents the volumetric change of the FS, A is the membrane area, and t is the time for the FO run. The reverse salt flux (RSF) was determined using equation 2.

$$Js = \frac{V_f C_f - V_i C_i}{A*t} \quad (2)$$

In equation 2, V_f and V_i are the final and initial volumes of the FS, respectively, C_f and C_i are the final and initial concentrations of the FS, respectively, A is the effective membrane area, and t is the filtration time. A conductivity metre obtained from LAQUA was used to record the change in the FS's conductivity, and a turbidity meter (Hach 2100P) was used for all turbidity measurements. Equation 3 was used to measure the pollutant rejection.

$$R = 1 - \frac{\frac{C_d V_d}{V_p}}{C_f} \quad (3)$$

In equation 3, C_d (ppm) is the concentration of the pollutants in the DS, V_d (L) represents the final volume of the DS, V_P (L) is the volume of the freshwater that permeated from the FS to the DS side, and C_f (ppm) is the initial pollutants concentration in the FS. The concentration of all the pollutants was measured using inductively coupled mass spectroscopy (ICP-MS).

2.4. FO fouling and cleaning experiments

A virgin pre-soaked TFC membrane was flushed with DI water for 30 minutes to remove any impurities and mounted in the FO filtration unit. Fouling studies were conducted in two membrane modes, the AL-FS and the AL-DS orientation. To obtain a normalisation factor for normalized flux, initial runs were conducted using deionized water (DI) feed and 0.6M NaCl DS. Following this, the FS was replaced with landfill leachate and the DS with a fresh 0.6 M NaCl DS. Short-term tests lasted four hours per cycle. After each cycle, the membrane was cleaned with a 30% H_2O_2 solution diluted with pure water to 3% on the fouled side and DI water on the other side. The landfill leachate wastewater has a neutral pH of 7.52 (Table 1), and hence no pH adjustments were made to the H_2O_2 solution in all experiments. Additionally, the primary aim of using H_2O_2 was to avoid by-products or to generate a secondary chemical waste stream. The addition of acid or bases to the H_2O_2 may generate reaction by-products, making the process less environmentally friendly.

Long filtration tests were performed in the AL-FS, with each cycle lasting 24 hours. Instead of a 0.6 M NaCl, a 1 M NaCl solution was the DS to avoid significant dilution of the NaCl DS. The FS and DS were changed after every 24 hours in the beginning of the new cycle. Cleaning in long-term experiments was conducted after every 24 hours, using DI water for the first few cycles and then with H_2O_2 to compare their efficiencies. The recovered water flux of the FO membrane was obtained mathematically using equation 4.

$$FR = \frac{J_c}{J_f} * 100 \quad (4)$$

J_f denotes the average flux of a fouled membrane over a complete period, while J_c denotes the flux of the membrane after cleaning.

2.5. Membrane tolerance tests for hydrogen peroxide

Active exposure tests were conducted to test the membrane tolerance to H_2O_2 oxidation. A pre-soaked TFC membrane was mounted on the FO cell to calculate the pure water flux and RSF as baseline results. DI water was used to wash the membrane for about 30 minutes to remove any accumulated salt. Then, the FS was changed to the H_2O_2 (50 ml/L of 30% solution diluted with 1 L of DI water) while DI water was on the other side to prevent membrane dehydration. The solution was circulated continuously and periodically stopped to record the pure water flux and RSF to compare them against the baseline values. The pure water flux and RSF were recorded after 1 hour and then periodically after every 4 hours. The membranes were considered damaged when there was a substantial variation in water transport or solute transport compared to the virgin membrane. Each trial was done twice to confirm the findings. The maximum dose of H_2O_2 the membrane could withstand was calculated using equation 5.

$$D_{max} = C * t_{max} \quad (5)$$

D_{max} (ppm-h) is the maximum dose of H_2O_2 the membrane could withstand before critical performance loss occurred (Ling et al., 2017), C is H_2O_2 concentration, and t_{max} is the maximum time the membrane could withstand the oxidant. Membrane specimens were dried (24 hours) then analysis and evaluated through microscopic analysis.

176 **2.6. Characterisation of FO membrane**

177 A Thermo Scientific Nicolet 6700 FT-IR spectrometer was used to perform Fourier transform
178 infrared (FT-IR) analysis to study the characterisation of virgin and long-term exposed
179 membranes to H_2O_2 over the range of 500–4000 cm^{-1}. All membranes were dried before
180 characterisation. Each scan was averaged from 50 scans. Microscopic analysis of the
181 membrane morphology was conducted using field emission scanning electron microscopy
182 (FE-SEM).

183 **2.7. Characteristics of the landfill leachate wastewater**

184 Inductively coupled plasma spectroscopy (Agilent Technologies ICP-MS 7900) was employed
185 to analyse the landfill leachate wastewater. All the samples were collected from the landfill
186 leachate containers with a plastic syringe. The colour of the leachate was a strong yellowish
187 brown Fig. S.1 (Supplementary information), representing refractory compounds in the
188 leachate formed by high concentrations of humic acids, fulvic acids, and hydrophilic fractions
189 (Ibrahim and Yaser, 2019; Marañón et al., 2010). The presence of iron can lead to inorganic
190 fouling that might contribute to irreversible fouling. The pH and conductivity were measured
191 with a meter supplied by AQUA. The humic acids were negatively charged at the measured
192 pH. The TOC (total organic carbon) values of the landfill leachate were measured using a TOC
193 analyser (Shimadzu Corporation, Japan).

194 **Table 1. Analysis of the landfill FS using ICP-MS**

Parameter	Value	Unit
Turbidity	35	NTU
Colour	Brown (yellowy)	
Apparent particles	Small particulates	
pH	7.52	-
Conductivity	12100	$\mu s.cm^{-1}$
Total dissolved solids	4500	mgL^{-1}
Total organic carbon	145.1±5	mgL^{-1}
Ammonia	<0.5	mgL^{-1}
Total suspended solids	27-117	mgL^{-1}

Total Iron	3.5-5.2	mgL^{-1}
Magnesium	95.3±5	mgL^{-1}
Calcium	126±5	mgL^{-1}
Potassium	47.87	mgL^{-1}

195

196 The wastewater treatment plant supplied the values of ammonia, total suspended solids,
197 and total iron.

198 **3. Results and discussions**

199 **3.1. FE-SEM and FT-IR Analysis of the fouled membranes**

200 To determine the best membrane orientation for dewatering the landfill leachate, initial
201 short-terms filtration tests were conducted to analyse the TFC membranes' performance in
202 the AL-DS and AL-FS modes using a 0.6M NaCl DS (simulating seawater osmotic pressure) and
203 landfill leachate FS. Detailed information of these tests is presented in supplementary
204 information (S.3.). The fouling mechanisms in the AL-FS and AL-DS modes were analysed using
205 the experimental data by plotting t/V vs V Fig. S.3.2 to evaluate whether fouling was mainly
206 because of the pore-blocking or cake formation mechanism (Wang and Tarabara, 2008). For
207 the AL-FS mode, the curves in Fig. S.3.2a show linear lines with a correlation coefficient almost
208 equal to 1, indicating that the cake layer in this orientation was the main cause of the small
209 decline in the flux over time. The FE-SEM analysis of the fouled active layer also revealed the
210 cake layer, as presented in Fig. S.3.2b. The cake layer in the AL-FS orientation from the FE-
211 SEM looks homogenous with a couple of cracks in the membrane. The cracks are due to the
212 process of drying the membrane before the FE-SEM analysis. The straight line in the plot (Fig
213 S3.2a) indicates a homogenous cake layer formation. The homogeneity of the cake layer was
214 probably due to the interactions between humic substances or polysaccharides with proteins
215 in the landfill leachate wastewater (Kim et al., 2014). It can be hypothesized that the cake
216 layer acts as a pre-filter, protecting the membrane from materials with high fouling propensity
217 in the landfill leachate wastewater (Di Bella and Di Trapani, 2019; Kochkodan et al., 2014).
218 This will ease cleaning the AL of the membrane and hence facilitate a high flux recovery.
219 However, the cake layer can also promote some foulants adsorption on the membrane
220 surface, which will be harder to remove by physical cleaning.

Compared to the AL-FS mode, the AL-DS mode water flux decline shows a curved line, indicating pore-blocking at the early stages of filtration, which is also evident from Fig S.3.1a the water flux declined rapidly in the first 75 minutes. The line seems to level out at the later stages of the experiment, showing that the flux decline shifted from pore-plugging to cake layer. The results are again in agreement with Fig S.3.1a, where the AL-DS water flux was stable. The FE-SEM of the fouled support layer is presented in Fig. S.3.2d; the red circle indicates large-sized fouling materials attached to the smaller foulants trapped inside the support layer. These foulants are possibly a combination of macromolecular (such as humic and fulvic acids, which are the major contributors to the organic fouling on the membrane) and soluble metal ions in the leachate wastewater (Mi and Elimelech, 2010).

The fouled membranes in both orientations were further examined through FT-IR spectroscopy to get some qualitative information about the foulants in the landfill leachate wastewater attached to the membrane surface. A visible change can be observed in the FT-IR of the fouled membrane (Fig. 1). Fig. 1a and 1b presented the FT-IR of pristine membrane and fouled membrane in the AL-FS orientation, respectively, and the FT-IR of the pristine membrane and the fouled membrane is presented in Fig 1c and 1d for the AL-DS mode. In the AL-FS mode, the FT-IR of the fouled membrane shows a small peak at the wavenumber 3749 cm^{-1}. This can be attributed to the clay particles (aluminium silicate) present in the landfill leachate wastewater. The clay particles were also visible in the landfill leachate wastewater (Fig. S.2). The band marked in the range 1520-1550 cm^{-1} and the peaks at 1481 and 1489 cm^{-1} represents secondary amide and indicate fouling due to proteins(Delaunay et al., 2008). The intensity at these bands shows a decrease in intensity compared to the pristine membrane. To gain more insights into the FT-IR of the foulants on the FO membrane, the fouled membrane spectra were subtracted from the pristine membrane spectra to get the spectra of the foulants only on the membrane surface. Spectral subtraction is frequently employed to isolate the spectral features of a component or physical change in the sample (Lin et al., 2001). The spectra of the foulants are presented in Fig. 1b for the AL-FS orientation treatment of the landfill.

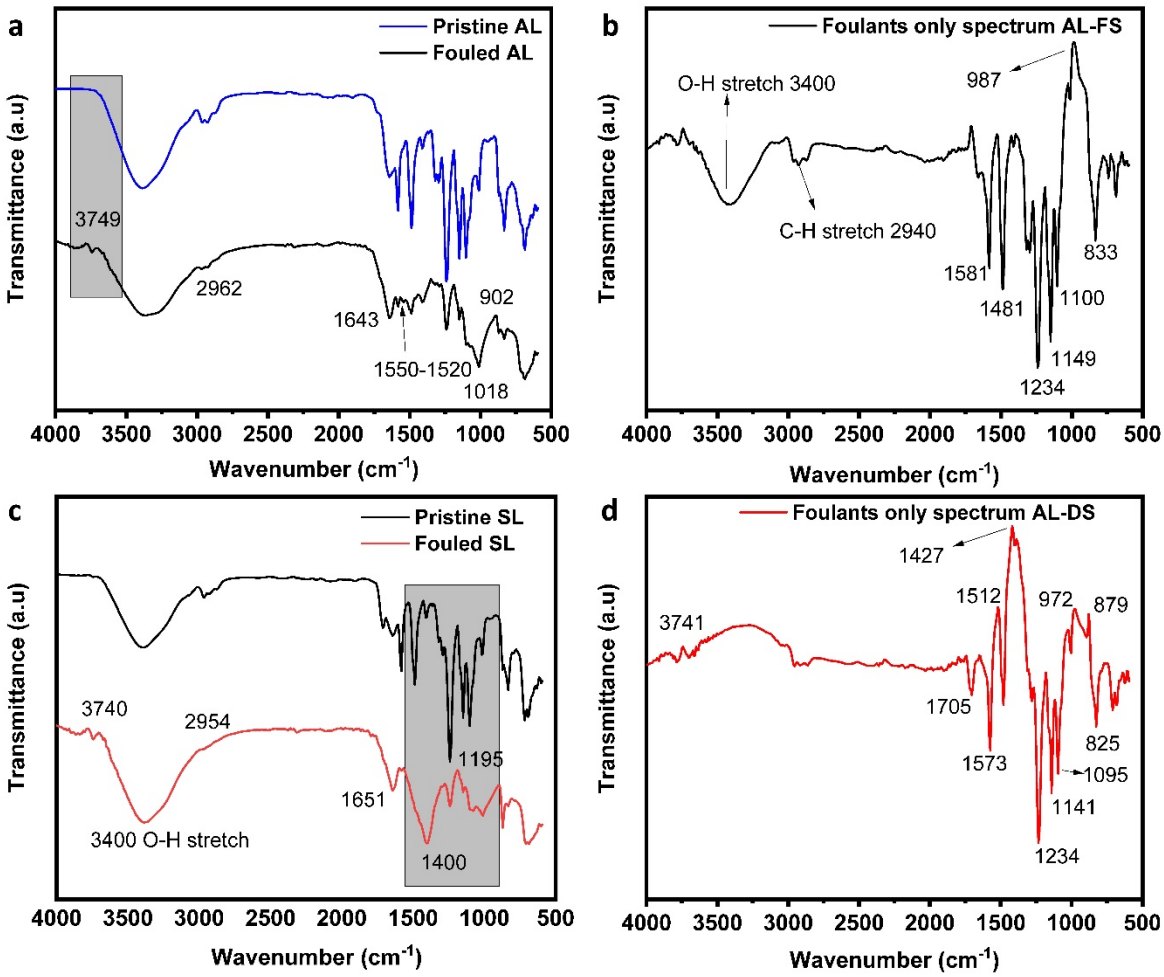

Figure 1: (a) FT-IR of the pristine active layer and fouled membrane operating in AL-FS orientation **(b)** FT-IR of the fouled active layer in the AL-FS orientation **(c)** FT-IR of the pristine support and fouled support layer of the membrane **(d)** FT-IR of the fouled support layer in the AL-DS mode.

The peak in the band 2940 cm^{-1} (Fig 1b) is an indicator of silica fouling (Nataraj et al., 2008). Silica fouling in the FO process can contribute to irreversible fouling (especially in the presence of divalent calcium and magnesium ions), as it is stubborn and hard to clean by physical cleaning methods such as hydraulic flushing. The peak at 1100 cm^{-1} is an indicator of the alcohol group. The FT-IR of the fouled FO membrane in the AL-DS orientation is presented in Fig. 1c and 1d. Fig. 1c compares the pristine membrane's spectrum with the fouled membrane, whereas Fig. 1d shows only the foulants spectrum. The band at 3400 cm^{-1} is attributed to the O-H groups. The AL-DS spectrum also shows the presence of clay particles (3741 $cm^{-1)}$ and silica fouling (2962 cm^{-1}). The bands in Fig. 1d from 1427-1600 are indicators

of aromatic compounds. The sharp peak at 1427 usually shows calcium carbonate scaling ($CaCO_3$) (Lee and Kim, 2009) due to Ca ions in the landfill leachate wastewater. The peak at this band is more intense when the FO membrane operates in the AL-DS orientation compared to the AL-FS. This implies that Ca ions have more fouling propensity in the AL-FS mode than the AL-DS mode. Both the AL-FS and the AL-DS fouled membrane showed similar peaks at 1234 cm^{-1}, associated with the carboxyl and ester group and primary and secondary amines (Croué et al., 2003; Kurtoğlu Akkaya and Bilgili, 2020).

3.2. Tolerance of FO membrane to H_2O_2 in extended exposure

A pre-soaked virgin TFC membrane was exposed to H_2O_2 at the cleaning concentration (50 ml/L) with the active layer facing the H_2O_2 solution, and DI water was circulated on the other side to avoid membrane dehydration. The concentration of H_2O_2 solution was chosen based on the previous studies (Ibrar et al., 2020a; Wang et al., 2017). Similar tests were conducted with the support layer against the H_2O_2 solution and DI water on the AL (active layer) side. After 24 hours, the H_2O_2 solution-DI water test was stopped, the membrane was cleaned with DI water (to flush out the H_2O_2) and a pure water flux and RSF were measured in the FO membrane using a 0.6M NaCl DS and DI water FS. The water flux and RSF were recorded every 4 hours during the experiment and presented in Fig. 2a and 2b. For the AL-FS orientation and the H_2O_2 facing the active layer, no major changes in the pure water flux and RSF were noticed until 72 hours. After 72 hours, the pure water flux of the TFC membrane using 0.6M NaCl DS and DI water reached 118 LMH (a fivefold increase compared to the baseline), demonstrating substantial damage to the membrane. Moreover, the RSF declined significantly at the breakdown point due to AL damage, and hence most of the water permeated across the membrane. This may also be a sign of membrane ageing due to the long exposure to oxidant (Benavente and Vázquez, 2004). Similar results of membrane damage after 72 hours of H_2O_2 exposure were reported by Abejón et al. (2013) for PA (polyamide) reverse osmosis membranes. However, the concentration of H_2O_2 was very high (35% w/w of aqueous H_2O_2 solution).

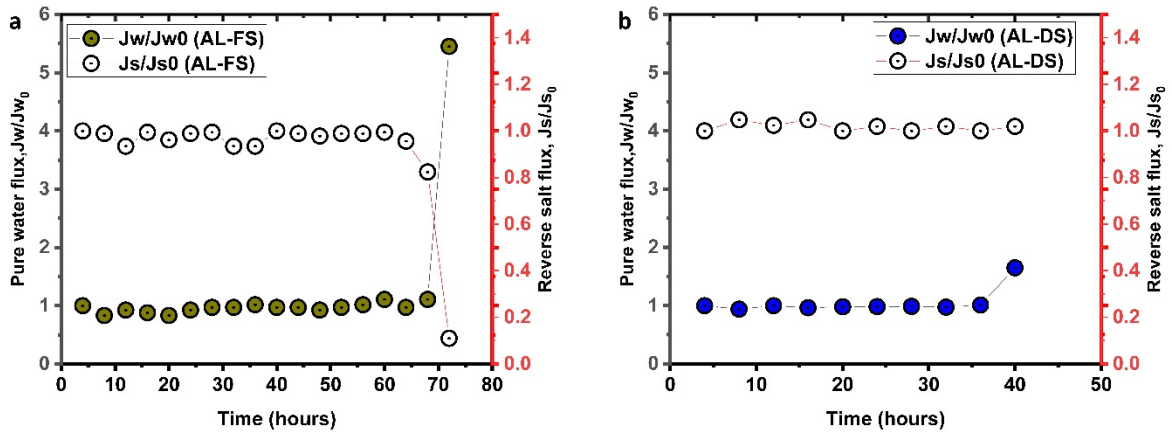

Figure 2: (a) Pure water flux and RSF recorded during the exposure tests, **(b)** Pure water flux and RSF recorded during the 40 hours exposure.

The support layer of the FO membrane tolerated the H_2O_2 concentration for 40 hours only before a significant change in performance was recorded. After 40 hours, the FO experiments showed a threefold increase in the pure water flux and no substantial change in the RSF than the virgin membrane. Most membrane manufacturers report oxidant exposure in terms of maximum tolerance dosage value or D_{max} (Abejón et al., 2013). The maximum H_2O_2 the membrane could withstand was calculated using equation [5]. Table 2 lists the maximum dosage calculated for the AL and the support layer (SL). All values were calculated at neutral pH. The polysulfone SL of the TFC membrane could tolerate the 3% concentration for only 40 hours during long-term exposure. A threefold increase in the pure water flux was recorded after 40 hours of operation only.

Table 2. Maximum dose values of hydrogen peroxide for the active layer and the support layer

Membrane Orientation	D_{max}	t_{max}	C
AL	3,600,000 ppm-h	72 hours	50,000 mg/L
SL	2,00,000 ppm-h	40 hours	50,000 mg/L

3.3. Characterization of the damaged membranes by FT-IR and FE-SEM

The exposed membranes exhibited significant changes in the transport properties, a sign of membrane performance deterioration. The degradation to the membranes was further confirmed by FT-IR analysis since no studies are available, which describes the oxidative damage of the FO membrane by FT-IR analysis. The pristine and exposed membranes were analysed through FT-IR spectroscopy to study the surface chemistry of the exposed membranes. Both the polyamide AL and the PSf SL FT-IR analysis were conducted and are presented for the active layer (Fig. 3a and 3 b) and the support layer (Fig. 3c and 3d).

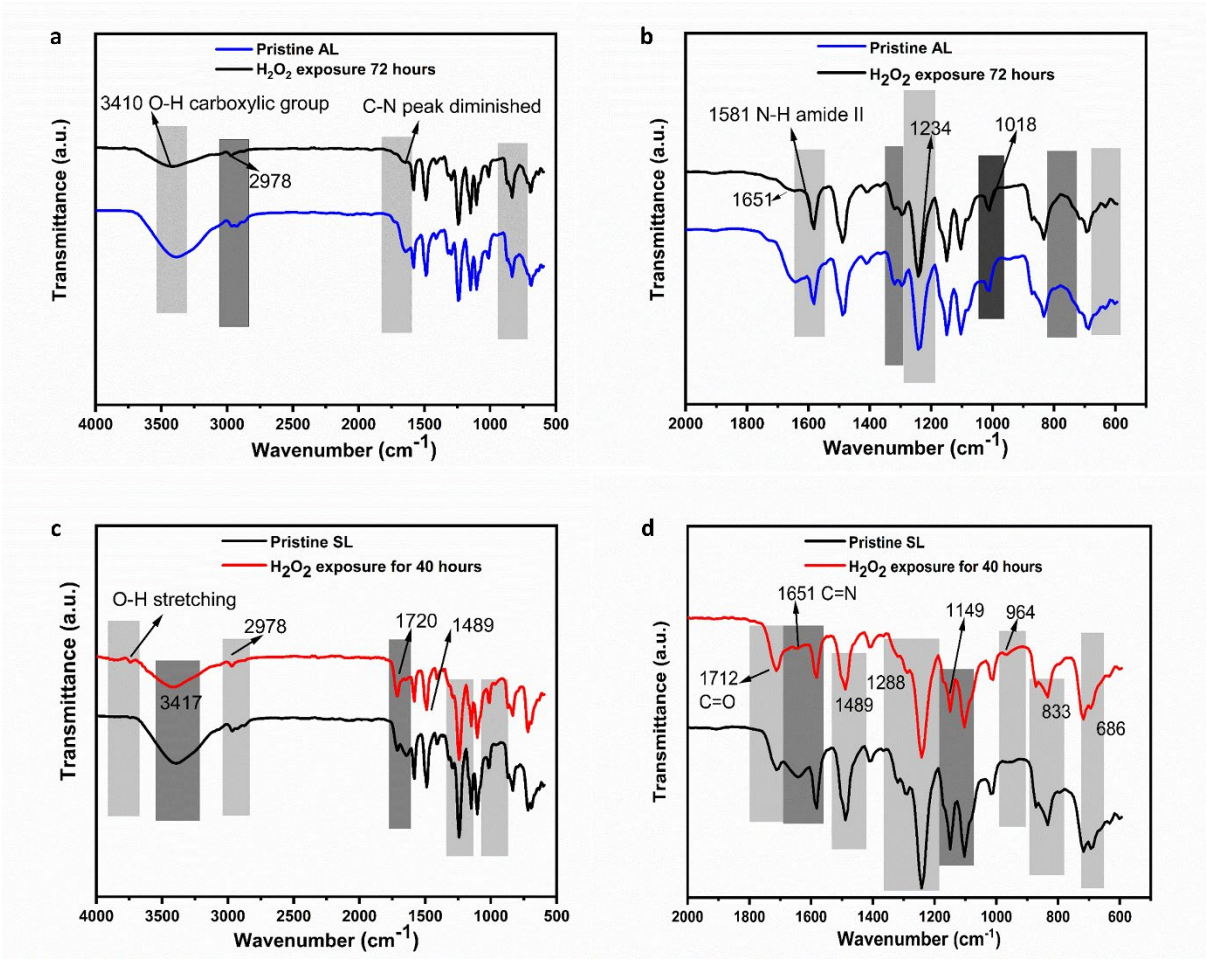

Figure 3: (a) FT-IR of the pristine active layer and exposed active layer of the membrane for 72 hours ranging from 4000 to 500 cm^{-1} **(b)** FT-IR of the pristine and exposed active layer of the membrane for 72 hours ranging from 2000 to 500 cm^{-1} **(c)** FT-IR of the pristine support and exposed support layer of the membrane for 42 hours ranging from 4000 to 500 cm^{-1} **(d)** FT-IR of the pristine and exposed support layer of the membrane for 40 hours ranging from 2000 to 500 cm^{-1}.

323 The most obvious disturbance in the spectra for the exposed AL was the suppression of the
324 peak intensity at 3400 cm^{-1}, indicating the O-H suppression (strong broad) of the carboxylic
325 group in the exposed membrane for 72 hours (Fig 3a). Similar peak suppression was observed
326 for the PSf SL exposed for 40 hours (Fig 3c). The ring suppression in these bands might cause
327 poor membrane performance in both orientations after continuous exposure to H_2O_2. There
328 was no change at the peak at wave number 3750 (O-H stretching alcohol) for the AL, but
329 suppression was visible in the SL at the same peak. For the damaged membranes, peak
330 suppression was observed at around 3000 cm^{-1}, as marked by the N-H stretching (amine salt)
331 for both the AL and the SL. Similar results were reported for oxidant-damaged polyamide RO
332 membranes by Antony et al. (2010). Minor suppression was also noticed for the O=C=O band
333 at around 2300 cm^{-1}. Significant stretching in the C=C band at around 1690 cm^{-1} indicates a
334 change in the hydrogen bonding behaviour for the AL. Suppression was visible for this peak
335 for the SL, suggesting a change in the hydrogen bonding behaviour for both the AL and the SL
336 and indicates poor membrane performance. A more visible spectrum for the FT-IR analysis
337 from wavenumber 2000–5000 cm^{-1} is provided in Fig. 3b and Fig. 3d for the AL and SL,
338 respectively. The peak at 1542 (N-H amide II) stands for the N-H plane bending (Antony et al.,
339 2010). Stretching was observed for the peak at 1664, indicating C=O stretching for the AL. This
340 peak is usually identified as amide I mode (Kwon et al., 2017). Stretching was noticed at this
341 band for the AL, as marked in Fig. 3b. Contrary to that observed for chlorine-damaged RO
342 membranes, the peak shifts in the AL for the N-H group were lesser than the stretching of the
343 C=O group. In general, H_2O_2 is known for reducing and oxidizing properties (Bienert et al.,
344 2006). For instance, H_2O_2 can oxidize the hydroxyl (-OH) group to the carbonyl ($R_2C=O$) group
345 (Sadri et al., 2014). Overall, it can be summarised that the oxidation of the membrane in the
346 long exposure tests leads to damage of the polar functional (hydroxyl, carbonyl and amide)
347 groups of the membrane.

348 The exposed membranes to H_2O_2 were further examined through FE-SEM analysis. The FE-
349 SEM of the pristine active layer of the TFC membrane (Fig. 4a and 4b). The FE-SEM of the
350 exposed active layer for 72 hours is also presented (Fig. 4c and 4d). The active layer after the
351 prolonged exposure to H_2O_2 appears to have scratches, possibly due to handling of the
352 membrane in preparation for FE-SEM analysis (Fig. 4c). However, no visible damage is

noticeable. At higher magnification (Fig. 4d), there is a considerable difference between the virgin and exposed membrane morphologies.

The FE-SEM of the pristine support layer (Fig. 4e and 4f) and exposed the support layer to H_2O_2 (Fig. 4g and 4h) were also examined. Compared to the AL, the SL FE-SEM shows clear visible signs of damage. Thus, the chemical cleaning of the SL with H_2O_2 is not recommended in the long term. Additional FE-SEM of the SL after 24 hours of exposure are also given in the supplementary information (S.4 Supplementary information). Although there was no significant change in the water flux or RSF after 24 hours, the FE-SEM of the support layer after 24 hours indicates cracks, indicating a change in the membrane morphology after 24 hours of exposure Fig. S.5.

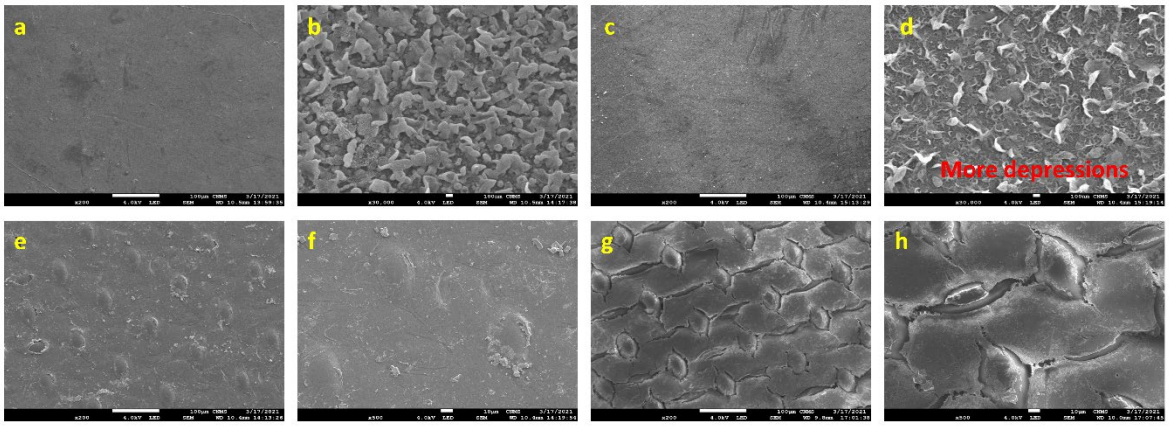

Figure 4 FE-SEM of the (**a)** pristine active layer at 100 µm; (**b)** pristine active layer at 100 nm**;** **(c)** exposed active layer toward H_2O_2 for 72 hours at 100 µm; **(d)** exposed active layer against H_2O_2 at 100 nm; (**e)** pristine support layer at 100 µm; (**f)** pristine support layer at 10 µm; **(g)** exposed support layer toward H_2O_2 for 40 hours at 100 µm; and **(h)** exposed support layer towards H_2O_2 at 10 µm.

3.4. Impact of membrane orientation on flux recovery

Laboratory tests were performed in both the membrane modes in consecutive cycles using a 0.6M NaCl DS to determine the best orientation for water reclamation from the landfill leachate. A cleaning cycle with H_2O_2 was conducted after each four-hour filtration cycle with landfill leachate. Table 3 and Fig. 5 show the flux recovery after each AL-DS and AL-FS filtration cycle. After the first filtration cycle, water flux recovery when the membrane AL against the

landfill leachate feed was 97.7±1 %. Then, the membrane was cleaned with H_2O_2 for 30 minutes and tested for landfill leachate filtration in another four-hour cycle to determine the impact of H_2O_2 cleaning in consecutive cycles. For the next three filtration cycles, the water flux recovery was 96.97±1 %, 92.9 %, and 84.95±1 %, respectively. The higher water flux recovery is due to the smooth surface of the active layer. It is also observed that there was no significant change in the RSF compared to the baseline RSF test. The AL-DS water flux recovery was 92±1% in the first cycle, followed by approximately 68±1% for cycle 2, 66±1% for cycle 3, and 61% for cycle 4. Based on the TFC membrane performance, the AL-FS can be selected as the best orientation for the landfill leachate dewatering under a long operating time.

Table 3. Flux recovery percentage in two membrane modes

Membrane orientation	Recovery Cycle-1 (%)	Recovery Cycle-2 (%)	Recovery Cycle-3 (%)	Recovery Cycle-4 (%)
AL-FS	97.74	96.97	92.9	84.95
AL-DS	92	68	66	61

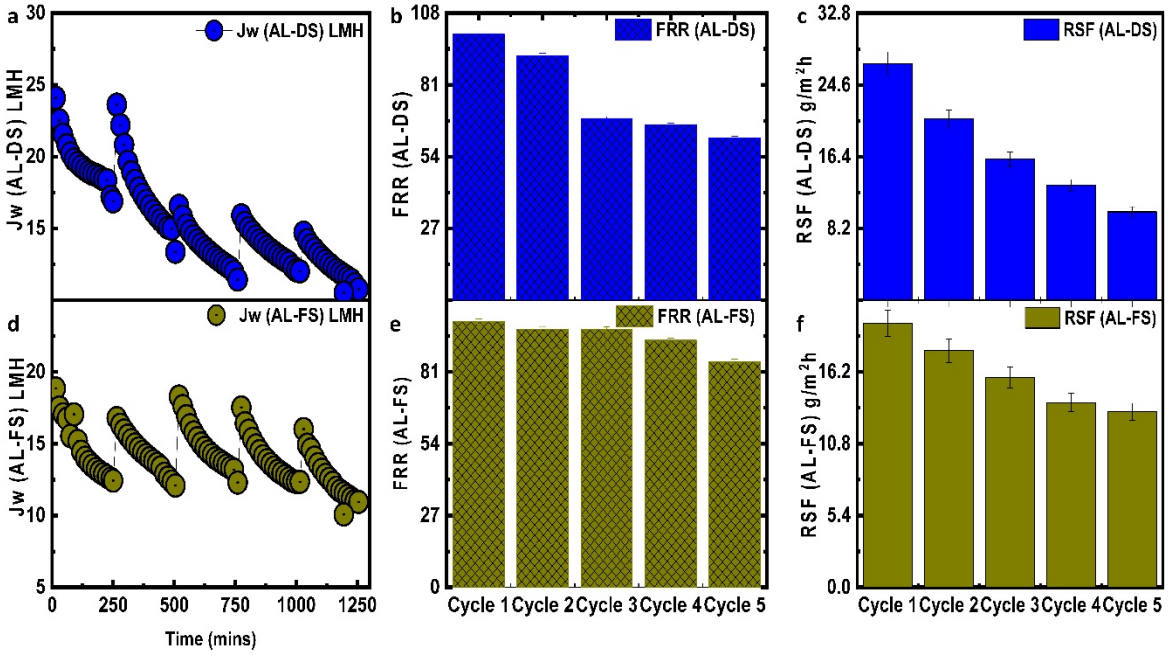

Figure 5 (a) Permeation flux in the AL-DS for five cycles **(b)** Flux recovery rate (FRR) in the AL-DS for five cycles after the initial baseline cycle **(c)** Plot of RSF in the AL-DS mode for the five cycles of filtration **(d)** AL-FS water flux in five cycles **(b)** AL-FS water flux recovery rate (FRR) for four cycles **(d)** Plot of RSF in the AL-DS for the four cycles of filtration.

The cleaning efficiency of the H_2O_2 cleaning for the AL-FS and the AL-DS orientation can be further elucidated by comparing the FT-IR of the pristine, fouled membrane by landfill leachate and cleaned membrane by H_2O_2. As evident from Fig.S.6 (Supplementary information), the band at 3749 cm^{-1} might be attributed to aluminosilicate, which is still present in the spectrum of the cleaned membrane with H_2O_2 in the AL-FS and the AL-DS mode. In principle, aluminosilicate or clay is resistant to chemical cleaning attack, high temperature, and pressures (Armstrong et al., 2009), and therefore H_2O_2 was not able to effectively remove the clay foulants. Interestingly, there is no difference in the intensity for this band in the AL-FS and the AL-DS mode. Proper pretreatment of the landfill leachate wastewater can eliminate clay particles or other colloids that may contribute to irreversible fouling on the membrane surface. The bands in the range 1520-1550 cm^{-1} and the peaks at 1481 and 1489 cm^{-1} for protein fouling in the cleaned membrane spectrum show great resemblance to that of the pristine membrane.

Results imply that H_2O_2 can be effectively employed for membrane cleaning fouled with a wide range of organic matters. Previous studies have also demonstrated that H_2O_2 can provide better cleaning efficiency than acid or alkaline cleaning. For instance, for PSf membranes fouled by glutamic acid wastewater, cleaning with H_2O_2 achieved higher water flux recovery than HCl and sodium hydroxide (NaOH) (Li et al., 2005). Also, for CTA membrane fouled by landfill wastewater, H_2O_2 cleaning was more effective than HCl cleaning and alkaline cleaning at pH 11 (Ibrar et al., 2020b). Other polysaccharides foulants (1034 cm^{-1}) are also effectively removed by the H_2O_2. The band at 1243 cm^{-1} (C-O-C stretching) for the cleaned membrane is identical in intensity to that of the pristine membrane. The peaks in this region are usually of phosphate groups (P=O from phosphate or C-O-P, P-O-P) associated with nucleic acids (Liu et al., 2015; Schmitt and Flemming, 1998). Other organic foulants (833 cm^{-1} to 686 cm^{-1}) are also effectively removed by the H_2O_2 as evident from the FT-IR in both the membrane orientations.

H_2O_2 is a green and cost-effective oxidising agent used to clean fouled wastewater membranes without generating any secondary by-products. H_2O_2 oxidises the foulants on the fouled membrane to carbon dioxide and water (Li et al., 2005). However, cleaning by H_2O_2 alone is a slow reaction, and the high content of some organic refractory compounds (Huang et al., 2020) or inorganic foulants (in this study) cannot be effectively removed at the used concentration and time.

3.5. Forward osmosis membrane performance in long filtration

While H_2O_2 can damage the membrane in long-term exposure, it is feasible to combine physical cleaning with an H_2O_2 chemical cleaning protocol for efficient FO operation. This will minimize the requirements for frequent membrane cleaning, reduce the damages associated with chemical cleaning, membrane integrity, and membrane lifetime, and reduce operational costs associated with chemical cleaning. Hence, long-term filtration tests were conducted using DI water physical cleaning and H_2O_2 chemical cleaning. Physical cleaning with DI water was done after the initial two cycles, and H_2O_2 was employed only in the last filtration cycle (Fig.6). It is noteworthy that all values of permeation flux were normalized to avoid the impact of dilution.

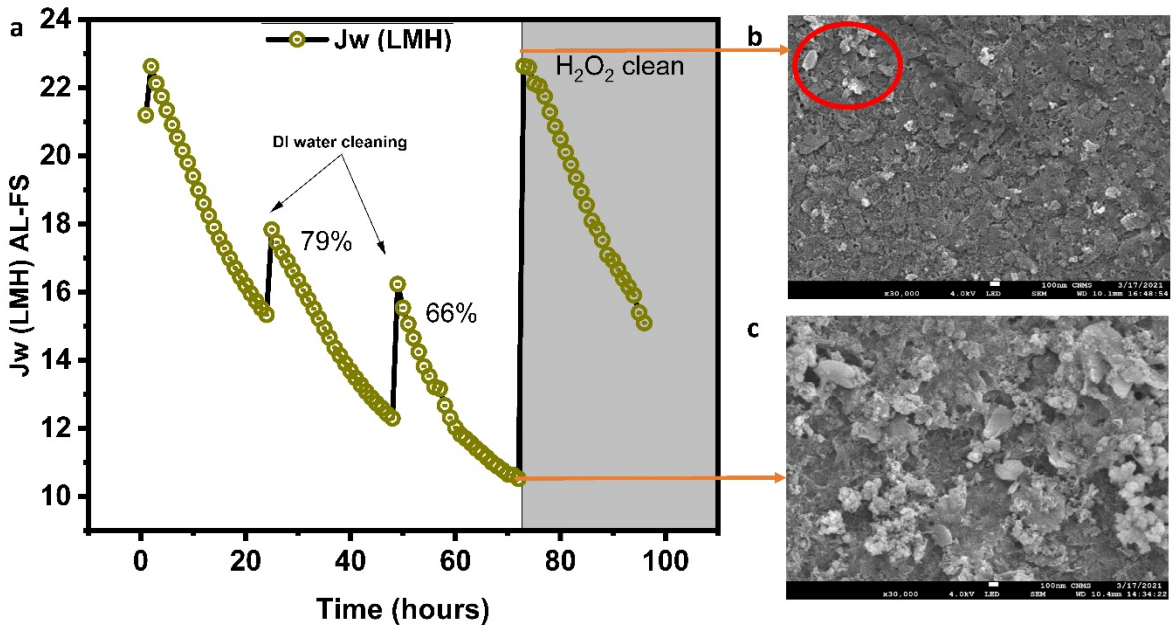

Figure 6: (a) Permeation flux in the AL-FS during long-term experiments, each cycle was 24 hours (**b)** FE-SEM analysis of the fouled membrane after the 72 hours filtration, (**c)** FE-SEM analysis of the membrane after cleaning with H2O2 after the 72 hours of filtration.

Since fouling in the AL-FS filtration style is governed by the cake layer, introducing some turbulence can dislodge fouling materials from the membrane surface. Physical cleaning at elevated cross-flow velocity (51 cm.sec^{-1}) was employed after each FO filtration cycle of 24-hour length. To avoid significant changes in the concentrations of the FS and DS, both were replenished after each 24-hour cycle. The high turbulence induced by physical cleaning with DI water only restored 79 ±1% (first cycle) and 66 ±1 % (second cycle) of the average water flux, indicating that some fouling materials were strongly attached to the membrane surface. This can be probably due to inorganic foulants such as silica foulants, which in the existence of Ca or Mg ions are stubbornly attached to the membrane and require chemical cleaning. It can also be assumed that physical cleaning could remove large-size fouling materials from the membrane surface, leaving the smaller and stubborn fouling matters. After 72 hours of FO filtration, H_2O_2 cleaning was employed, which restored 92 ± 2 % of the average flux. The FE-SEM of the fouled membrane before 72 hours of filtration is shown in Fig. 6b. After 72 hours of filtration by H_2O_2 (Fig. 6c), the cleaned membrane showed some irreversible fouling (red circle), which is still attached to the membrane surface. This seems like inorganic scaling, which is inevitable due to the complex nature of the landfill leachate wastewater. In this study, the inorganic scaling on the membrane is mainly caused by the clay particles (3741 cm$^{-1)}$ and silica fouling (2962 cm^{-1}), as presented earlier in the FT-IR. It is evident from the FE-SEM and FT-IR analysis that H_2O_2 concentration and duration were insufficient to remove the irreversible inorganic scaling of the membrane effectively. Proper pretreatment of the landfill leachate wastewater can be another effective way to control inorganic fouling. Also, antiscalant blended DS or lowering FS pH would reduce inorganic scaling in long-term FO operations (Zhang et al., 2017).

The TFC membrane achieved efficient rejection for total organic carbon (98 %) and turbidity of 99.5% as presented in Fig. S.6. The rejection of divalent calcium and magnesium ions was higher than the rejection of monovalent potassium. This can be attributed to the larger hydrated radii and smaller crystal radii of calcium and magnesium ions compared to the potassium ion (Tansel et al., 2006). Generally, it is important to take inorganic scaling into account when selecting proper cleaning protocols. Since flushing with DI water combined with H_2O_2 cleaning was not completely effective for removing inorganic scaling, the osmotic backwash method could be coupled with H_2O_2 and proven effective (Ibrar et al., 2020b).

Future research should investigate combining the osmotic backwashing method with the H_2O_2 method to clean organic and inorganic foulants as an environmentally friendly method.

4. Conclusions

FO can be a viable alternative for dewatering landfill leachate; it can efficiently reject contaminants in landfill leachate wastewater. In short-term filtration cycles, cleaning with H_2O_2 proved to be an efficient cleaning protocol in the AL-FS filtration style. However, only 70% of the average flux could be restored in the AL-DS filtration style. This study also explored long-term exposure of TFC membrane to H_2O_2 cleaning. The AL of the FO membrane could tolerate the cleaning concentration in this study for almost 72 hours, whereas the support layer could only tolerate it for about 40 hours. Both the AL and the SL were damaged after the long-term exposure, as confirmed from the FT-IR and FE-SEM analysis. For efficient FO operation, physical cleaning protocols such as DI water flushing or osmotic backwashing techniques should be combined with chemical cleaning with H_2O_2 to avoid compromising the membrane integrity. Future studies should test the forward osmosis membrane's tolerance to other cleaning agents or wastewater laden with chemicals. Additionally, novel chemical cleaning protocols, which can clean the membrane without compromising integrity, should be investigated.

Acknowledgement

We are thankful to the Australian government by providing scholarship support to Ibrar.

References

Abbas, A.A., Jingsong, G., Ping, L.Z., Ya, P.Y., Al-Rekabi, W.S., 2009. Review on LandWll Leachate Treatments. Journal of Applied Sciences Research 5, 534-545.

Abejón, R., Garea, A., Irabien, A., 2013. Effective Lifetime Study of Commercial Reverse Osmosis Membranes for Optimal Hydrogen Peroxide Ultrapurification Processes. Industrial & Engineering Chemistry Research 52, 17270-17284.

Aftab, B., Ok, Y.S., Cho, J., Hur, J., 2019. Targeted removal of organic foulants in landfill leachate in forward osmosis system integrated with biochar/activated carbon treatment. Water Research 160, 217-227.

Antony, A., Fudianto, R., Cox, S., Leslie, G., 2010. Assessing the oxidative degradation of polyamide reverse osmosis membrane—Accelerated ageing with hypochlorite exposure. Journal of Membrane Science 347, 159-164.

Armstrong, M.W., Gallego, S., Chesters, S.P., 2009. Cleaning clay from fouled membranes. Desalination and Water Treatment 10, 108-114.

Atmaca, E., 2009. Treatment of landfill leachate by using electro-Fenton method. Journal of Hazardous Materials 163, 109-114.

506 Benavente, J., Vázquez, M.I., 2004. Effect of age and chemical treatments on characteristic
507 parameters for active and porous sublayers of polymeric composite membranes. Journal of
508 Colloid and Interface Science 273, 547-555.
509 Bhol, P., Yadav, S., Altaee, A., Saxena, M., Misra, P.K., Samal, A.K., 2021. Graphene-Based
510 Membranes for Water and Wastewater Treatment: A Review. ACS Applied Nano Materials.
511 Bienert, G.P., Schjoerring, J.K., Jahn, T.P., 2006. Membrane transport of hydrogen peroxide.
512 Biochimica et Biophysica Acta (BBA)-Biomembranes 1758, 994-1003.
513 Cai, W., Liu, J., Zhang, X., Ng, W.J., Liu, Y., 2016. Generation of dissolved organic matter
514 and byproducts from activated sludge during contact with sodium hypochlorite and its
515 implications to on-line chemical cleaning in MBR. Water Research 104, 44-52.
516 Croué, J.-P., Benedetti, M., Violleau, D., Leenheer, J., 2003. Characterization and copper
517 binding of humic and nonhumic organic matter isolated from the South Platte River: evidence
518 for the presence of nitrogenous binding site. Environmental Science & Technology 37, 328-
519 336.
520 Danley-Thomson, A., Worley-Morse, T., Contreras, S.U.J., Herman, S., Brawley, A., Karcher,
521 K., 2020. Determining the effects of Class I landfill leachate on biological nutrient removal in
522 wastewater treatment. Journal of Environmental Management 275, 111198.
523 Delaunay, D., Rabiller-Baudry, M., Gozálvez-Zafrilla, J.M., Balannec, B., Frappart, M.,
524 Paugam, L., 2008. Mapping of protein fouling by FTIR-ATR as experimental tool to study
525 membrane fouling and fluid velocity profile in various geometries and validation by CFD
526 simulation. Chemical Engineering and Processing: Process Intensification 47, 1106-1117.
527 Di Bella, G., Di Trapani, D., 2019. A Brief Review on the Resistance-in-Series Model in
528 Membrane Bioreactors (MBRs). Membranes 9, 24.
529 Dong, Y., Wang, Z., Zhu, C., Wang, Q., Tang, J., Wu, Z., 2014. A forward osmosis membrane
530 system for the post-treatment of MBR-treated landfill leachate. Journal of Membrane Science
531 471, 192-200.
532 Farooque, A.M., Al-Amoudi, A., Numata, K., 1999. Degradation study of cellulose triacetate
533 hollow fine-fiber SWRO membranes. Desalination 123, 165-171.
534 Ghanbari, F., Wu, J., Khatebasreh, M., Ding, D., Lin, K.-Y.A., 2020. Efficient treatment for
535 landfill leachate through sequential electrocoagulation, electrooxidation and
536 PMS/UV/CuFe2O4 process. Separation and Purification Technology 242, 116828.
537 Huang, J., Luo, J., Chen, X., Feng, S., Wan, Y., 2020. How Do Chemical Cleaning Agents Act
538 on Polyamide Nanofiltration Membrane and Fouling Layer? Industrial & Engineering
539 Chemistry Research 59, 17653-17670.
540 Ibrahim, A., Yaser, A.Z., 2019. Colour removal from biologically treated landfill leachate with
541 tannin-based coagulant. Journal of Environmental Chemical Engineering 7, 103483.
542 Ibrar, I., Yadav, S., Altaee, A., Hawari, A., Nguyen, V., Zhou, J., 2020a. A novel empirical
543 method for predicting concentration polarization in forward osmosis for single and
544 multicomponent draw solutions. Desalination 494, 114668.
545 Ibrar, I., Yadav, S., Altaee, A., Samal, A.K., Zhou, J.L., Nguyen, T.V., Ganbat, N., 2020b.
546 Treatment of biologically treated landfill leachate with forward osmosis: Investigating
547 membrane performance and cleaning protocols. Science of The Total Environment 744,
548 140901.
549 Iskander, S.M., Novak, J.T., He, Z., 2019. Reduction of reagent requirements and sludge
550 generation in Fenton's oxidation of landfill leachate by synergistically incorporating forward
551 osmosis and humic acid recovery. Water Research 151, 310-317.
552 Kim, Y., Elimelech, M., Shon, H.K., Hong, S., 2014. Combined organic and colloidal fouling
553 in forward osmosis: Fouling reversibility and the role of applied pressure. J. Membr. Sci. 460,
554 206-212.

555 Kochkodan, V., Johnson, D.J., Hilal, N., 2014. Polymeric membranes: Surface modification
556 for minimizing (bio)colloidal fouling. Advances in Colloid and Interface Science 206, 116-140.
557 Kurtoğlu Akkaya, G., Bilgili, M.S., 2020. Evaluating the performance of an electro-membrane
558 bioreactor in treatment of young leachate. Journal of Environmental Chemical Engineering 8,
559 104017.
560 Kwon, S.J., Park, S.-H., Park, M.S., Lee, J.S., Lee, J.-H., 2017. Highly permeable and
561 mechanically durable forward osmosis membranes prepared using polyethylene lithium ion
562 battery separators. Journal of Membrane Science 544, 213-220.
563 Lee, M., Kim, J., 2009. Membrane autopsy to investigate CaCO3 scale formation in pilot-scale,
564 submerged membrane bioreactor treating calcium-rich wastewater. Journal of Chemical
565 Technology & Biotechnology 84, 1397-1404.
566 Li, F., Wichmann, K., Heine, W., 2009. Treatment of the methanogenic landfill leachate with
567 thin open channel reverse osmosis membrane modules. Waste Management 29, 960-964.
568 Li, K., Li, S., Huang, T., Dong, C., Li, J., Zhao, B., Zhang, S., 2019. Chemical Cleaning of
569 Ultrafiltration Membrane Fouled by Humic Substances: Comparison between Hydrogen
570 Peroxide and Sodium Hypochlorite. International Journal of Environmental Research and
571 Public Health 16, 2568.
572 Li, X., Li, J., Fu, X., Wickramasinghe, R., Chen, J., 2005. Chemical cleaning of PS ultrafilters
573 fouled by the fermentation broth of glutamic acid. Separation and Purification Technology 42,
574 181-187.
575 Lin, C.-F., Liu, S.-H., Hao, O.J., 2001. Effect of functional groups of humic substances on UF
576 performance. Water research 35, 2395-2402.
577 Ling, R., Yu, L., Pham, T.P.T., Shao, J., Chen, J.P., Reinhard, M., 2017. The tolerance of a
578 thin-film composite polyamide reverse osmosis membrane to hydrogen peroxide exposure.
579 Journal of Membrane Science 524, 529-536.
580 Liu, Y., Chang, S., Defersha, F.M., 2015. Characterization of the proton binding sites of
581 extracellular polymeric substances in an anaerobic membrane bioreactor. Water Research 78,
582 133-143.
583 Marañón, E., Castrillón, L., Fernández-Nava, Y., Fernández-Méndez, A., Fernández-Sánchez,
584 A., 2010. Colour, turbidity and COD removal from old landfill leachate by coagulation-
585 flocculation treatment. Waste management & research 28, 731-737.
586 Marttinen, S., Kettunen, R., Sormunen, K., Soimasuo, R., Rintala, J., 2002. Screening of
587 physical–chemical methods for removal of organic material, nitrogen and toxicity from low
588 strength landfill leachates. Chemosphere 46, 851-858.
589 Mi, B., Elimelech, M., 2010. Organic fouling of forward osmosis membranes: Fouling
590 reversibility and cleaning without chemical reagents. Journal of Membrane Science 348, 337-
591 345.
592 Nataraj, S., Schomäcker, R., Kraume, M., Mishra, I.M., Drews, A., 2008. Analyses of
593 polysaccharide fouling mechanisms during crossflow membrane filtration. Journal of
594 Membrane Science 308, 152-161.
595 Nguyen, T.-T., Kook, S., Lee, C., Field, R.W., Kim, I.S., 2019. Critical flux-based membrane
596 fouling control of forward osmosis: Behavior, sustainability, and reversibility. Journal of
597 Membrane Science 570-571, 380-393.
598 Peng, Y., 2017. Perspectives on technology for landfill leachate treatment. Arabian Journal of
599 Chemistry 10, S2567-S2574.
600 Rautenbach, R., Mellis, R., 1994. Waste water treatment by a combination of bioreactor and
601 nanofiltration. Desalination 95, 171-188.
602 Renou, S., Givaudan, J., Poulain, S., Dirassouyan, F., Moulin, P., 2008a. Landfill leachate
603 treatment: Review and opportunity. Journal of hazardous materials 150, 468-493.

Renou, S., Givaudan, J.G., Poulain, S., Dirassouyan, F., Moulin, P., 2008b. Landfill leachate treatment: Review and opportunity. Journal of Hazardous Materials 150, 468-493.
Reshadi, M.A.M., Bazargan, A., McKay, G., 2020. A review of the application of adsorbents for landfill leachate treatment: Focus on magnetic adsorption. Science of The Total Environment 731, 138863.
Sadri, F., Ramazani, A., Massoudi, A., Khoobi, M., Tarasi, R., Shafiee, A., Azizkhani, V., Dolatyari, L., Joo, S.W., 2014. Green oxidation of alcohols by using hydrogen peroxide in water in the presence of magnetic Fe3O4 nanoparticles as recoverable catalyst. Green Chemistry Letters and Reviews 7, 257-264.
Schmitt, J., Flemming, H.-C., 1998. FTIR-spectroscopy in microbial and material analysis. International Biodeterioration & Biodegradation 41, 1-11.
Tansel, B., Sager, J., Rector, T., Garland, J., Strayer, R.F., Levine, L., Roberts, M., Hummerick, M., Bauer, J., 2006. Significance of hydrated radius and hydration shells on ionic permeability during nanofiltration in dead end and cross flow modes. Separation and Purification Technology 51, 40-47.
Trebouet, D., Schlumpf, J.P., Jaouen, P., Quemeneur, F., 2001. Stabilized landfill leachate treatment by combined physicochemical–nanofiltration processes. Water Research 35, 2935-2942.
Wang, F., Tarabara, V.V., 2008. Pore blocking mechanisms during early stages of membrane fouling by colloids. Journal of Colloid and Interface Science 328, 464-469.
Wang, X., Hu, T., Wang, Z., Li, X., Ren, Y., 2017. Permeability recovery of fouled forward osmosis membranes by chemical cleaning during a long-term operation of anaerobic osmotic membrane bioreactors treating low-strength wastewater. Water Research 123, 505-512.
Wang, Z., Tang, J., Zhu, C., Dong, Y., Wang, Q., Wu, Z., 2015. Chemical cleaning protocols for thin film composite (TFC) polyamide forward osmosis membranes used for municipal wastewater treatment. Journal of Membrane Science 475, 184-192.
Yadav, S., Ibrar, I., Altaee, A., Samal, A.K., Ghobadi, R., Zhou, J., 2020a. Feasibility of brackish water and landfill leachate treatment by GO/MoS2-PVA composite membranes. Sci. Total Environ., 141088.
Yadav, S., Saleem, H., Ibrar, I., Naji, O., Hawari, A.A., Alanezi, A.A., Zaidi, S.J., Altaee, A., Zhou, J., 2020b. Recent developments in forward osmosis membranes using carbon-based nanomaterials. Desalination 482, 114375.
Zhang, M., She, Q., Yan, X., Tang, C.Y., 2017. Effect of reverse solute diffusion on scaling in forward osmosis: A new control strategy by tailoring draw solution chemistry. Desalination 401, 230-237.